coatings

Article

Impact of Throughflow and Coriolis Force on the Onset of Double-Diffusive Convection with Internal Heat Source

Kallu Vetty Muhammed Rafeek [1], Gudala Janardhana Reddy [1,*], Ravi Ragoju [2], Gundlapally Shiva Kumar Reddy [2] and Mikhail A. Sheremet [3,4,*]

1 Laboratory on Computational Fluid Dynamics, Department of Mathematics, Central University of Karnataka, Kalaburagi 585367, Karnataka, India; rafeekkv997@gmail.com
2 Department of Applied Sciences, National Institute of Technology Goa, Ponda 403401, Goa, India; ravi@nitgoa.ac.in (R.R.); gshivakumarreddy913@gmail.com (G.S.K.R.)
3 Laboratory on Convective Heat and Mass Transfer, Tomsk State University, 634050 Tomsk, Russia
4 Butakov Research Center, National Research Tomsk Polytechnic University, 634050 Tomsk, Russia
* Correspondence: gjr@cuk.ac.in (G.J.R.); sheremet@math.tsu.ru (M.A.S.)

Abstract: The present research examines the joint influence of throughflow and Coriolis force on the onset of double-diffusive convection with an internal heat source modelled by Darcy's law. The BVP4C routine in MATLAB R2020a is used to solve the eigenvalue problem numerically. Critical Rayleigh numbers are obtained for designated values of governing parameters. The effect of the internal heat source parameter, Taylor number, Darcy number, and Peclet number on the system's stability is investigated. The internal heat source parameter has a destabilizing influence on the system, according to our findings. The reason behind this observation is that the presence of an internal heat source in the porous medium may cause more molecular diffusion inside the medium. The Taylor number, on the other hand, stabilizes the system for both upward and downward throughflow because rotation introduces vorticity into the fluid. Thus, the fluid moves with higher velocity in horizontal planes. The velocity of the fluid perpendicular to the planes reduces as a result of this motion. Thus, the onset of convection is delayed.

Keywords: porous medium; internal heat source; throughflow; rotation

check for updates

Citation: Rafeek, K.V.M.; Reddy, G.J.; Ragoju, R.; Reddy, G.S.K.; Sheremet, M.A. Impact of Throughflow and Coriolis Force on the Onset of Double-Diffusive Convection with Internal Heat Source. *Coatings* **2022**, *12*, 1096. https://doi.org/10.3390/coatings12081096

Academic Editor: Hadj Benkreira

Received: 10 April 2022
Accepted: 28 July 2022
Published: 2 August 2022

1. Introduction

Convection with an internal heat source has been of interest to many researchers, since it has extensive applications in astrophysics [1], combustion modelling [2], geophysics [3], the miniaturization of electronic components [4] and thermal ignition [5]. Non-linear temperature circulation in the system is steered by the presence of an internal heat source, and convection may occur. Tritton and Zarraga [6] conducted the first experimental research on internally heated thermal convection, which was followed by theoretical studies by Roberts [7] and Thirby [8]. The origins of this phenomenon were established by Tveitereid and Palm [9]. Takashima ([10,11]) explored convection in a biased fluid layer with internal heat. They discovered that an inner heat source has a significant impact on the stability of the onset of convection. Natural convection affected by the heat source with the outcome of heat source distribution was tested by Tasaka and Takeda [12]. The analysis of free convection in a porous medium plays a substantial role in many areas, such as geophysical systems, the Earth's oceans, magma chambers, the petroleum industry and many engineering applications. Nield and Bejan [13] provided a brief review of this topic.

There are many studies related to geophysical sciences and technological applications which contain non-isothermal motion of liquids, known as throughflow. With the height of the fluid, this flow transforms the basic state temperature equation from linear to non-linear, altering the system's stability. Jones and Persichetti [14] discussed the thermal instability in packed beds with throughflow. Wooding [15] studied the Rayleigh instability of a thermal boundary layer flow in saturated porous medium, in which he showed that the layer is stable provided that the Rayleigh number for the system does not exceed a critical positive value and that the wave number of the critical neutral disturbance is finite. Homsy and Sherwood [16] investigated the linear and energy theory on thermal instability in porous media with throughflow. They showed that the fluid can lose stability through either a buoyantly driven mode or through a continuous analogue of the Saffman–Taylor mode. Sutton [17] and Shivakumara [18] explored the impact of throughflow on the onset of convection in a horizontal porous layer.

The effect of throughflow and internal heat generation on the onset of convection in a porous material was examined by Khalili and Shivakumara [19]. They concluded that, if the boundaries are of the same type, throughflow destabilizes the system, but this is not true when internal heat source is absent. In a porous material with a tilted temperature drop and vertical throughflow, Brevdo [20] described 3D absolute and convective instability at the onset of convection. He deduced the fact that for marginally supercritical values of the vertical Rayleigh number, the destabilization has the character of absolute instability in all of the cases in which the horizontal Rayleigh number is zero or the Peclet number is zero. Shivakumara and Sureshkumar [21] investigated convective instability in non-Newtonian fluids in vertical throughflow, and concluded that throughflow has an essential influence depending on the nature of the borders and fluid flow directions. Yadav [22] scrutinized the impacts of throughflow and a varied gravity field on the onset of convective flow in a porous medium layer numerically by employing the higher order Galerkin method, and showed that both the throughflow and gravity variation parameters postpone the onset of convective motion. Later, many researchers such as Kiran [23], Bhadauria and Kiran [24], Kiran [25], Shinkumara and Nanjundappa [26], Reza and Gupta [27], Nield and Kuznetsov [28], Yadav [29] and Kiran and Bhadauria [30] investigated the effect of throughflow with different external effects.

Convection driven by the internal heating of porous material was investigated by Gasser and Kazimi [31] and Tveitereid [32]. Yadav et al. [33] performed linear analysis and used the Galerkin method to explain the onset of convection in rotating porous media with an inner heater. Mahabaleshwar et al. [34] analyzed the convection heat transfer in a porous zone with modulated gravity and an inner heater. Some interesting results can be found in [35–37].

Riahi [38] investigated nonlinear convection in a porous region with an inner heater and discovered that the non-uniform internal heat source could reduce or enhance the ideal Rayleigh value and cell size. In the case of linear and nonlinear stability, Rionero and Straughan [39] derived a critical Rayleigh value. The internal heat-generating porous medium in vertical cavities was investigated by Du and Bilgen [40]. Hewitt et al. [41] overworked the underlying theory, mechanism, correlations and methodologies of heat transfer. Choi et al. [42] investigated a variety of characteristics of convection flow in porous medium caused and prolonged by a constant inner heater. Brinkman convection in a rotating porous zone filled with a nanofluid with an inner heater was investigated by Yadav et al. [43]. An internal heater's influence on the onset of convection in a porous medium filled with a nanosuspension was studied by Yadav et al. [44]. Barletta et al. [45] studied the influence of viscous dissipation in the porous material. The stability of mixed thermal convection in a porous zone was discussed by Sphaier et al. [46] using the generalized integral transform technique. The effects of inner thermal production and throughflow on convective instability in an anisotropic porous medium were studied by Vanishree [47].

The present paper aims to study the thermal convection stability with an internal heater in porous material. The plan of this research is as follows. In Section 2, we describe the considered problem. In Section 3, we discuss the basic state. In Section 4, the linear instability analysis is performed. The method of solution is described in Section 5. The numerical outcomes and discussions are presented in Section 6. The research ends with conclusions.

2. Governing Equations

We consider heat conducting liquid in a porous zone placed between two infinitely parallel horizontal plates at $z = 0$ and $z = L$ which are set to rotate at a fixed angular velocity $\overline{\Omega} = \Omega\bar{e}_z$. The upper and lower bounding surfaces of the layer are assumed to be stress-free. The z-axis is oriented upward, so that $g' = -g'\bar{e}_z$ where g' is the modulus of g' and $\bar{e}_z$ is the unit vector along the z-direction in Figure 1. Physical properties of the fluid are assumed to be constant, except density in the buoyancy term, so that the Boussinesq approximation is valid. The control Oberbeck–Boussinesq equations are [48]:

$$\nabla \cdot \mathrm{u} = 0 \tag{1}$$

$$\mathrm{u} = -\nabla P + Da\nabla^2\mathrm{u} + Ra\theta\bar{e}_z + \sqrt{Ta}(\mathrm{u} \times \bar{e}_z) \tag{2}$$

$$\frac{\partial\theta}{\partial t} + (u\cdot\nabla)\theta = \nabla^2\theta + Q \tag{3}$$

with the following boundary conditions

$$\begin{aligned} u = 0, \theta = 1 \text{ on } z = 0 \\ u = \theta = 0 \text{ on } z = 1. \end{aligned} \tag{4}$$

where u is the velocity, t is the time, θ is the temperature, Da is the Darcy number, Ra is the Rayleigh number, Ta is the Taylor number and Q is the parameter of inner heater, defined as follows:

$$Da = \frac{\mu_e}{\mu}\frac{K}{L^2}, Ra = \frac{\rho_0 g\beta\Delta T L^3}{\alpha\cdot\mu}, Q = \frac{Q' L^2}{k\Delta T}, Ta = \left(\frac{2\rho_0\Omega_0 K}{\mu\cdot\phi}\right)^2, \ P = \frac{K}{\alpha\cdot\mu}\left(\overline{P} + \rho_0 g z^*\right).$$

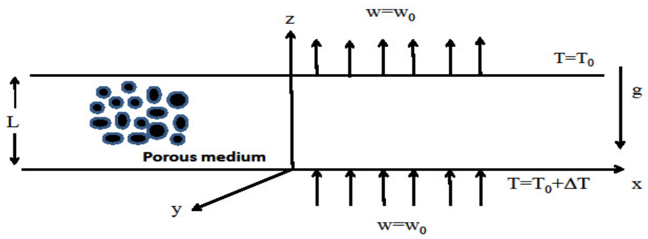

Figure 1. Schematic of the problem.

The rescaling used to obtain Equations (1)–(3) with conditions (4) is

$$(x, y, z) = \left(\frac{x^*}{L}, \frac{y^*}{L}, \frac{z^*}{L}\right), (u, v, w) = \left(\frac{Lu^*}{\alpha}, \frac{Lv^*}{\alpha}, \frac{Lw^*}{\alpha}\right), t = \frac{\alpha}{L^2 A}t^*, \alpha = \frac{k}{(\rho c_p)_f}, \tag{5}$$

where asterisks refer to dimensional quantities, L is the channel height, A is the ratio of volumetric thermal capacity of liquid filled porous material to the fluid, i.e., $A = \frac{(\rho c)_m}{(\rho c_p)_f}$, α is the thermal diffusivity, k is the thermal conductivity, K is the permeability, ρ_0 is the mean flow density, μ is the dynamic viscosity, ϕ is the porosity, ω is the angular velocity, μ_e is the effective viscosity, $Q' > 0$ is a (fixed) inner heater and β is the thermal expansion coefficient.

3. Basic State

The basic steady motion of Equations (1)–(3) is defined by a uniform throughflow,

$$u_b = 0, v_b = 0, w_b = Pe \tag{6}$$

where b stands for the basic state, $Pe = \frac{w_0 L}{\alpha}$ is the Peclet number and w_0 is the prescribed vertical throughflow velocity. The Peclet number is positive for upward throughflow and negative for downward throughflow. By substituting Equation (6) into Equation (3), we obtain the basic temperature profile as

$$\theta_b = \frac{e^{zPe} - e^{Pe}}{1 - e^{Pe}} + \frac{\left(z + e^{zPe} - ze^{Pe} - 1\right)Q}{\left(1 - e^{Pe}\right)Pe} \tag{7}$$

4. Linear Stability Study

The perturbation of the basic state can be defined as

$$u = u_b + \varepsilon u', \theta = \theta_b + \varepsilon\theta', P = P_b + \varepsilon P'. \tag{8}$$

where $\varepsilon \ll 1$. By substituting Equation (8) into Equations (1)–(4) and by neglecting terms $O\left(\varepsilon^2\right)$ or higher, we obtain the linearized governing equations as follows:

$$u' = -\nabla\overline{P'} + Da\nabla^2 u' + Ra\theta'\bar{e}_z + \sqrt{Ta}\left(u' \times \bar{e}_z\right) \tag{9}$$

$$\frac{\partial\theta'}{\partial t} + F(z)w' + Pe\frac{\partial\theta}{\partial z} = \nabla^2\theta' \tag{10}$$

$$w' = \theta' = 0 \text{ at } z = 0,\ 1 \tag{11}$$

where $F(z) = \frac{Q}{Pe} + \frac{e^{zPe}(Pe+Q)}{\left(1-e^{Pe}\right)}$. By taking the third components of the curl of (9) and the double curl of (9), we obtain

$$\left(1 - Da\nabla^2\right)\omega_z - \sqrt{Ta}\frac{\partial w}{\partial z} = 0 \tag{12}$$

$$\left(1 - Da\nabla^2\right)\nabla^2 w' - Ra\nabla_h^2\theta' + \sqrt{Ta}\frac{\partial\omega_z}{\partial z} = 0 \tag{13}$$

where $\omega_z = (\nabla \times u')\hat{e}_z$. By removing ω_z from Equations (12) and (13), one obtains

$$\left(1 - Da\nabla^2\right)^2\nabla^2 w' - Ra\left(1 - Da\nabla^2\right)\nabla_h^2\theta' + Ta\frac{\partial^2 w'}{\partial z^2} = 0 \tag{14}$$

Normal modes can be defined by the perturbations

$$\left(w', \theta'\right) = (W(z), \theta(z))e^{i(mx+ly)+\sigma t} \tag{15}$$

where $q = (m, l, 0)$ is the wave vector, with $q = \sqrt{m^2 + l^2}$ expressing the wave number, and σ is a complex characteristic, where its real part, σ_r, is the raising rate of instability and its imaginary part, σ_i, is the angular frequency. Substituting the above expression into Equations (10) and (14), we obtain:

$$\left(1 - Da\left(D^2 - q^2\right)\right)^2\left(D^2 - q^2\right)W + Ra\left(1 - Da\left(D^2 - q^2\right)\right)q^2\theta + Ta \cdot D^2 W = 0 \tag{16}$$

$$\left(D^2 - q^2 - PeD - i\omega\right)\theta - W \cdot F(z) = 0 \tag{17}$$

$$W = D^2 W = D^4 W = \theta = 0 \text{ on } z = 0,\ 1. \tag{18}$$

The principle of exchange of stabilities is used. In other words, the marginal stability condition can be found for stationary modes. Hence, Equations (16)–(18) become

$$\left(1 - Da\left(D^2 - q^2\right)\right)^2\left(D^2 - q^2\right)W + Ra\left(1 - Da\left(D^2 - q^2\right)\right)q^2\theta + Ta \cdot D^2 W = 0 \tag{19}$$

$$\left(D^2 - q^2 - PeD\right)\theta - W \cdot F(z) = 0 \tag{20}$$

$$W = D^2W = D^4W = \theta = 0 \text{ on } z = 0,\ 1. \quad (21)$$

5. Solution Methodology

The eigenvalue problem, defined by Equations (19)–(21), is worked out by employing the BVP4C routine in MATLAB R2020a. To achieve a non-trivial solution to the eigenvalue problem, the normalizing condition $w'(0) = 1$ is considered. We compute the eigenvalue Ra using this normalization condition. The critical Rayleigh and wave numbers are acquired by using index-linked instruction in MATLAB R2020a. The comparative and conclusive patience were taken as 10^{-6} and 10^{-10} independently to achieve higher-order exactness.

6. Results and Discussion

This section contains the numerical results and discussions. A numerical study of the eigenvalue problem corresponding to a convection problem with the uniform internal heat source and throughflow was performed in this paper. The non-dimensional parameters governing the onset of convection are the Rayleigh number, Ra, inner heater parameter, Q, Taylor number, Ta, Darcy number, Da, and Peclet number, Pe. The BVP4C routine in Matlab R2020a is used to work out the eigenvalue problem for linear stability analysis.

We verified our results with those found in the literature to validate our analysis method. In the absence of throughflow and rotation, the current problem reduces to that of Gasser and Kazimi [31] for Darcy porous media. Table 1 demonstrates that our numerical results are really close to Gasser and Kazimi's critical external Rayleigh number. Furthermore, the current numerical results are validated by comparing them to those found by Barletta et al. [48] for Q = 0, Ta = 0 and Da = 0 (see Table 2).

Table 1. Critical Rayleigh number values for Ta = 0; Da = 0 and Pe = 0 compared with [31].

Q	Gasser and Kazimi [31]	Present Study
0	39.48	39.4788
5	34.59	34.5953
10	27.02	27.0162
15	21.45	21.4436
20	17.63	17.6267
25	14.92	14.9165
30	12.91	12.9117
40	10.16	10.1606
50	8.37	8.3690
60	7.11	7.1121
80	5.47	5.4670
100	4.44	4.4391

Table 3 illustrates the Rayleigh number critical values for various Q and Pe, for constant Da = 0.01, Da = 0.1, and Ta = 50. A graphical representation of these values is given in Figure 2. The results for upward throughflow are shown in Figure 2. The Ra_c reduces with a growth of Q in this figure, suggesting that the internal heat source parameter has a destabilizing influence on the system. The reason behind this observation is that the presence of an internal heat source in the porous medium may cause more molecular diffusion inside the medium.

Table 4 shows the Ra_c for different Q and Pe, along with fixed Da = 0.01, Da = 0.1 and Ta = 50. Figure 3 illustrates a visual behavior of these values. The results for downward throughflow are shown in Figure 3. As can be seen in this figure, the critical Rayleigh number reduces as Q increases, implying that Q has a destabilizing influence on the system.

Table 2. Critical Rayleigh number values for $Q = 0$; $Ta = 0$ and $Da = 0$ compared with [48].

Pe	Barletta et al. [48]	Present Study	Pe	Barletta et al. [48]	Present Study
−0.001	39.4784	39.47842	0.001	39.4784	39.47842
−0.01	39.4786	39.47856	0.01	39.4786	39.47856
−0.1	39.4924	39.49237	0.1	39.4924	39.49237
−1	40.8751	40.87507	1	40.8751	40.87507
−2	45.0776	45.07761	2	45.0776	45.07761
−3	52.0684	52.06842	3	52.0684	52.06842
−4	61.6664	61.66642	4	61.6664	61.66642
−5	73.4146	73.41456	5	73.4146	73.41456
−6	86.6192	86.61920	6	86.6192	86.61920
−7	100.581	100.58085	7	100.581	100.58085
−8	114.833	114.83260	8	114.833	114.83260
−9	129.167	129.16685	9	129.167	129.16685
−10	143.518	143.51849	10	143.518	143.51849
−15	215.283	215.28280	15	215.283	215.28280

Table 3. Critical Rayleigh number for upward throughflow fixed at $Ta = 50$.

Q	$Da = 0.01$			$Da = 0.1$		
	$Pe = 0.001$	$Pe = 0.01$	$Pe = 0.1$	$Pe = 0.001$	$Pe = 0.01$	$Pe = 0.1$
1	470.7949	470.8283	471.2445	360.2181	360.2767	360.9591
2	456.8040	456.8651	457.5531	353.1931	353.3036	354.5031
3	436.5979	436.6802	437.5732	342.6116	342.7646	344.3875
4	413.2066	413.3041	414.3438	329.7012	329.8865	331.8297
5	389.0000	389.1083	390.2508	315.5820	315.7903	317.9600
6	365.4518	365.5675	366.7803	301.1062	301.3299	303.6501
7	343.3180	343.4387	344.6974	286.8434	287.0766	289.4889
8	322.8993	323.0231	324.3092	273.1351	273.3735	275.8350
9	304.2439	304.3692	305.6686	260.1618	260.4023	262.8818
10	287.2738	287.3996	288.7016	247.9998	248.2401	250.7157
11	271.8562	271.9817	273.2784	236.6618	236.9005	239.3566
12	257.8414	257.9660	259.2515	226.1242	226.3602	228.7861
13	245.0812	245.2044	246.4745	216.3440	216.5764	218.9648
14	233.4375	233.5590	234.8107	207.2690	207.4974	209.8434
15	222.7858	222.9053	224.1365	198.8445	199.0685	201.3693
16	213.0155	213.1329	214.3422	191.0165	191.2360	193.4896
17	204.0293	204.1446	205.3312	183.7335	183.9484	186.1542
18	195.7422	195.8553	197.0187	176.9479	177.1581	179.3200
19	188.0798	188.1907	189.3307	170.6157	170.8213	172.9315
20	180.9771	181.0857	182.2025	164.6970	164.8982	166.9615

The behavior of Ra_c versus the Taylor number is shown in Table 5 and Figure 4. Figure 4 shows that as the Taylor number rises, the critical Rayleigh number rises as well, indicating the stabilizing impact of the Taylor number. This can be explained as follows: rotation introduces vorticity into the fluid. Thus the fluid moves in horizontal planes with higher velocity. On account of this motion, the velocity of the fluid perpendicular to the planes reduces. Thus, the onset of convection is delayed.

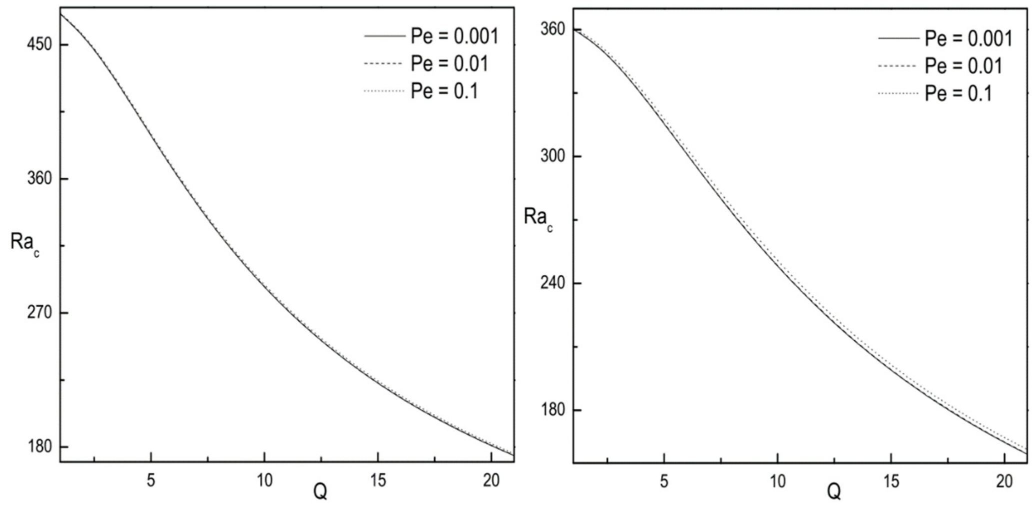

(**a**) (**b**)

Figure 2. Dependence of Ra_c on Q for (**a**) Da = 0.01 and (**b**) Da = 0.1.

Table 4. Critical Rayleigh number for downward throughflow fixed at Ta = 50.

Q	Da = 0.01			Da = 0.1		
	Pe = −0.001	Pe = −0.01	Pe = −0.1	Pe = −0.001	Pe = −0.01	Pe = −0.1
1	470.7877	470.7561	470.5231	360.2053	360.1488	359.6803
2	456.7906	456.7312	456.2149	353.1688	353.0604	352.0715
3	436.5798	436.4992	435.7636	342.5778	342.4269	341.0094
4	413.1850	413.0890	412.1932	329.6602	329.4769	327.7328
5	388.9761	388.8691	387.8591	315.5359	315.3296	313.3517
6	365.4262	365.3117	364.2219	301.0567	300.8349	298.6994
7	343.2913	343.1717	342.0281	286.7918	286.5603	284.3257
8	322.8720	322.7493	321.5716	273.0823	272.8456	270.5550
9	304.2162	304.0919	302.8952	260.1085	259.8696	257.5545
10	287.2460	287.1211	285.9168	247.9465	247.7077	245.3905
11	271.8285	271.7039	270.5004	236.6089	236.3718	234.0684
12	257.8139	257.6902	256.4938	226.0720	225.8375	223.5590
13	245.0539	244.9316	243.7470	216.2925	216.0615	213.8155
14	233.4106	233.2900	232.1205	207.2184	206.9914	204.7831
15	222.7593	222.6405	221.4885	198.7949	198.5722	196.4048
16	212.9894	212.8727	211.7397	190.9678	190.7496	188.6251
17	204.0038	203.8892	202.7763	183.6859	183.4722	181.3917
18	195.7171	195.6047	194.5126	176.9012	176.6922	174.6559
19	188.0552	187.9450	186.8739	170.5701	170.3656	168.3734
20	180.9530	180.8450	179.7950	164.6525	164.4525	162.5039

Table 5. Critical Rayleigh number for upward throughflow fixed at Q = 2.

Ta	Da = 0.01			Da = 0.1		
	Pe = 0.001	Pe = 0.01	Pe = 0.1	Pe = 0.001	Pe = 0.01	Pe = 0.1
5	111.6703	111.7037	112.0815	148.2322	148.3047	149.0853
10	162.3775	162.4197	162.8861	180.1151	180.1960	181.0679
15	207.2615	207.3097	207.8364	207.7227	207.8099	208.7501
20	248.5374	248.5894	249.1605	232.6185	232.7106	233.7058
25	287.2261	287.2787	287.8852	255.5851	255.6815	256.7225
30	323.9144	323.9714	324.6015	277.0832	277.1830	278.2636
35	358.9829	359.0413	359.6915	297.4115	297.5145	298.6298
40	392.6975	392.7571	393.4230	316.7779	316.8836	318.0299
45	425.2544	425.3149	425.9932	335.3336	335.4418	336.6159
50	456.8040	456.8651	457.5531	353.1931	353.3036	354.5031
55	487.4646	487.5261	488.2217	370.4458	370.5583	371.7811
60	517.3322	517.3939	518.0952	387.1627	387.2771	388.5215
65	546.4853	546.5471	547.2528	403.4019	403.5180	404.7824
70	574.9901	575.0518	575.7605	419.2113	419.3290	420.6121
75	602.9020	602.9637	603.6743	434.6310	434.7502	436.0508

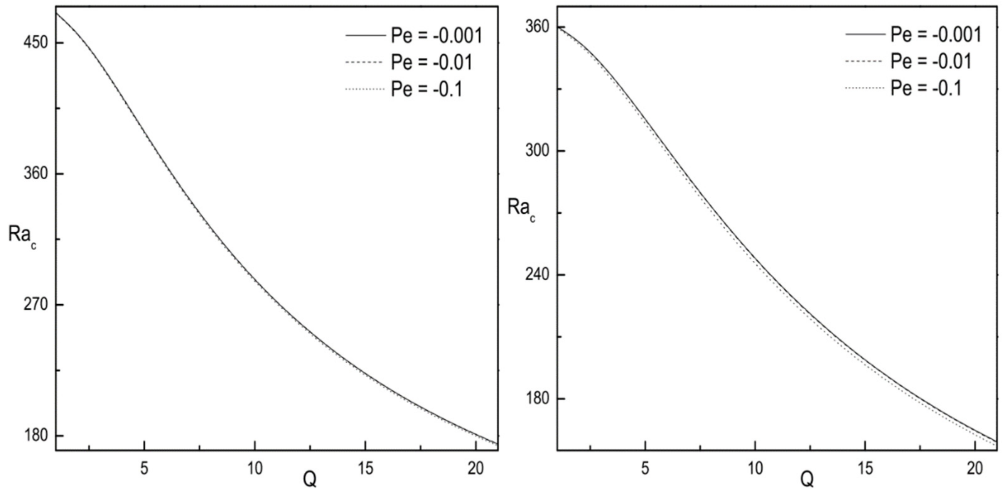

(**a**) (**b**)

Figure 3. Dependence of Ra_c on Q for (**a**) Da = 0.01 and (**b**) Da = 0.1.

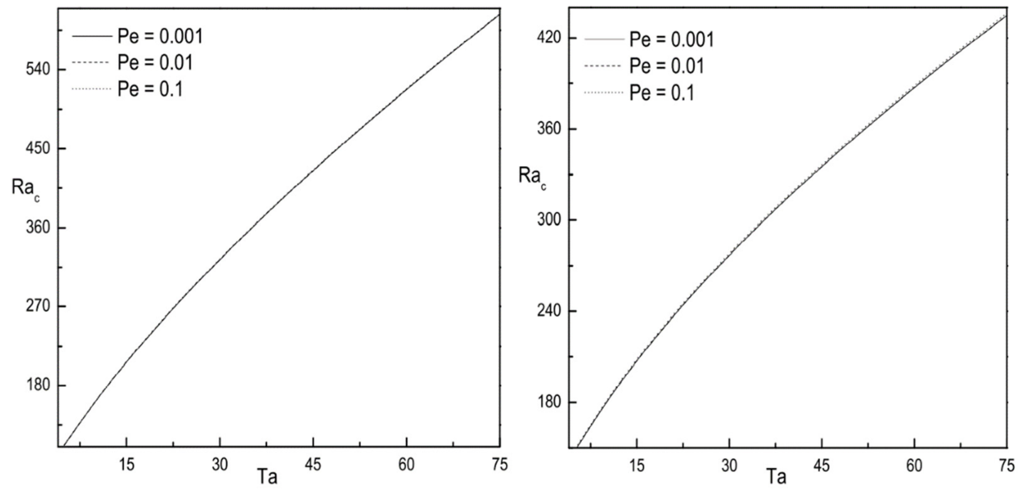

(**a**) (**b**)

Figure 4. Dependence of Ra_c on Ta for (**a**) Da = 0.01 and (**b**) Da = 0.1.

Table 6 and Figure 5 show the dependence of Ra_c on Ta for various Pe. Only the results for downward throughflow are shown in this part. The critical Rayleigh number rises with the increase in Ta, as shown in Figure 5, indicating that the Taylor number has a stabilizing impact.

Table 6. Critical Rayleigh number for downward throughflow fixed at Q = 2.

Ta	*Da* = 0.01			*Da* = 0.1		
	$Pe = -0.001$	$Pe = -0.01$	$Pe = -0.1$	$Pe = -0.001$	$Pe = -0.01$	$Pe = -0.1$
5	111.6629	111.6289	111.3183	148.2162	148.1449	147.4869
10	162.3681	162.3262	161.9452	180.0972	180.0177	179.2843
15	207.2509	207.2037	206.7770	207.7035	207.6178	206.8289
20	248.5259	248.4750	248.0171	232.5982	232.5076	231.6749
25	287.2114	287.1590	286.6808	255.5639	255.4693	254.6004
30	323.9019	323.8463	323.3516	277.0612	276.9631	276.0635
35	358.9700	358.9130	358.4081	297.3889	297.2878	296.3616
40	392.6844	392.6263	392.1149	316.7546	316.6508	315.7013
45	425.2412	425.1823	424.6673	335.3097	335.2036	334.2333
50	456.7906	456.7312	456.2149	353.1688	353.0604	352.0715
55	487.4512	487.3915	486.8757	370.4210	370.3107	369.3048
60	517.3187	517.2588	516.7450	387.1375	387.0254	386.0041
65	546.4718	546.4120	545.9013	403.3764	403.2626	402.2272
70	574.9766	574.9167	574.4103	419.1854	419.0700	418.0217
75	602.8885	602.8289	602.3276	434.6048	434.4880	433.4276

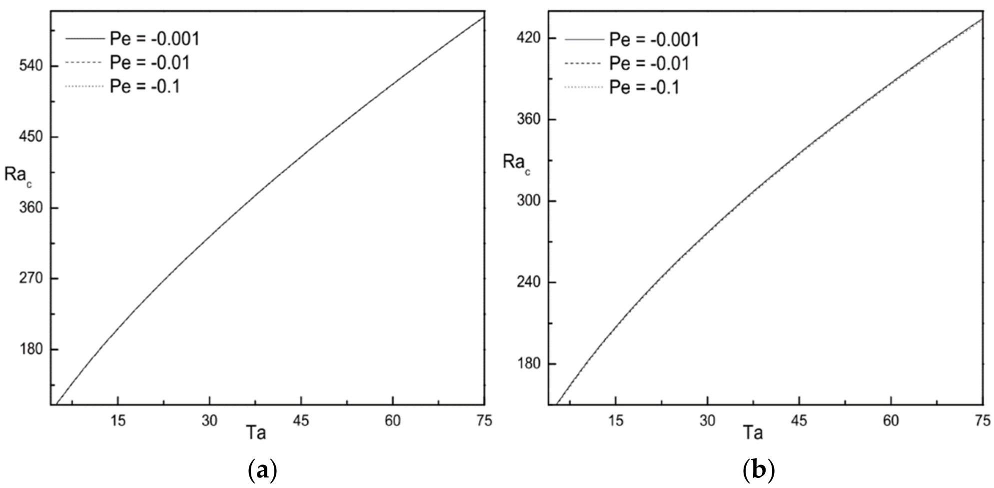

Figure 5. Dependence of Ra_c on *Ta* for (**a**) *Da* = 0.01 and (**b**) *Da* = 0.1.

7. Conclusions

This study has examined the linear instability of rotation convection in a porous zone with an inner heater. The behavior of various parameters such as the inner heater coefficient Q, critical Rayleigh number Ra_c, Peclet number *Pe*, Taylor number *Ta*, and Darcy number *Da* has been analyzed. The following are the most important findings from the linear instability:

- In the absence of throughflow and rotation, the Ra_c and the wave number for the Darcy porous medium match with those found in the literature and reported by Gasser and Kazimi [31].
- In the absence of an inner heater and rotation, the critical values of *Ra* for the Darcy porous medium are identical to those discovered by Barletta et al. [48].
- The system is destabilized by the internal heat source parameter.
- The Taylor number has a stabilizing impact on the considered unit for both upward and downward throughflows.

Author Contributions: Conceptualization, G.J.R.; methodology, K.V.M.R., G.J.R. and R.R.; software, R.R. and G.J.R.; writing—original draft preparation, K.V.M.R., G.J.R., R.R., G.S.K.R. and M.A.S.; writing—review and editing, K.V.M.R., G.J.R., R.R., G.S.K.R. and M.A.S.; visualization, K.V.M.R., G.J.R. and R.R. All authors have read and agreed to the published version of the manuscript.

Funding: The first author wishes to express his gratitude to the Department of Science and Technology, Government of India for the granting of DST-Inspire Fellowship (IF190169) (Grant no. C/4084/IFD/2020-21) and to the Central University of Karnataka for providing the research facilities. This research of the fifth author was supported by the Tomsk Polytechnic University Development Programme (Priority-2030-NIP/EB-002-0000-2022).

Institutional Review Board Statement: Not applicable.

Informed Consent Statement: Not applicable.

Data Availability Statement: All data can be found in this paper.

Acknowledgments: The authors are grateful to editor and anonymous referees for their suggestions and comments that helped in the enhancement of the clarity and depth of the interpretation of the results in the paper.

Conflicts of Interest: The authors declare no conflict of interest.

References

1. Tritton, D.J. Internally heated convection in the atmosphere of Venus and in the laboratory. *Nature* **1975**, *257*, 110–112. [CrossRef]
2. Hurley, M.J.; Gottuk, D.T.; Hall, J.R., Jr.; Harada, K.; Kuligowski, E.D.; Puchovsky, M.; Watts, J.M., Jr.; Wieczorek, C.J. (Eds.) *SFPE Handbook of Fire Protection Engineering*; Springer: Berlin/Heidelberg, Germany, 2015.
3. Mckenzie, D.P.; Roberts, J.M.; Weiss, N.O. Convection in the Earth's mantle: Towards a numerical simulation. *J. Fluid Mech.* **1974**, *62*, 465–538. [CrossRef]
4. Chadwick, M.L.; Webb, B.W.; Heaton, H.S. Natural convection from two-dimensional discrete heat sources in a rectangular enclosure. *Int. J. Heat Mass Transf.* **1991**, *34*, 1679–1693. [CrossRef]
5. May, H.O. A numerical study on natural convection in an inclined square enclosure containing internal heat sources. *Int. J. Heat Mass Transf.* **1991**, *34*, 919–928. [CrossRef]
6. Tritton, D.J.; Zarraga, M.N. Convection in horizontal layers with internal heat generation. Experiments. *J. Fluid Mech.* **1967**, *30*, 21–31. [CrossRef]
7. Roberts, P.H. Convection in horizontal layers with internal heat generation. Theory. *J. Fluid Mech.* **1967**, *30*, 33–49. [CrossRef]
8. Thirlby, R. Convection in an internally heated layer. *J. Fluid Mech.* **1970**, *44*, 673–693. [CrossRef]
9. Tveitereid, M.; Palm, E. Convection due to internal heat sources. *J. Fluid Mech.* **1976**, *76*, 481–499. [CrossRef]
10. Takashima, M. The stability of natural convection in an inclined fluid layer with internal heat generation. *J. Phys. Soc. Jpn.* **1989**, *58*, 4431–4440. [CrossRef]
11. Takashima, M. The stability of natural convection in an inclined fluid layer with internal heat generation. II. *J. Phys. Soc. Jpn.* **1991**, *60*, 455–465. [CrossRef]
12. Tasaka, Y.; Takeda, Y. Effects of heat source distribution on natural convection induced by internal heating. *Int. J. Heat Mass Transf.* **2005**, *48*, 1164–1174. [CrossRef]
13. Nield, D.A.; Bejan, A. *Convection in Porous Media*, 3rd ed.; Springer: New York, NY, USA, 2013.
14. Jones, M.C.; Persichetti, J.M. Convective instability in packed beds with throughflow. *AIChE J.* **1986**, *32*, 1555–1557. [CrossRef]
15. Wooding, R.A. Rayleigh instability of a thermal boundary layer in flow through a porous medium. *J. Fluid Mech.* **1960**, *9*, 183–192. [CrossRef]
16. Homsy, G.M.; Sherwood, A.E. Convective instabilities in porous media with throughflow. *AIChE J.* **1976**, *22*, 168–174. [CrossRef]
17. Sutton, F.M. Onset of convection in a porous channel with net throughflow. *Phys. Fluids* **1970**, *13*, 1931. [CrossRef]
18. Shivakumara, I.S. Effects of throughflow on convection in porous media. *Proc. Seventh Asian Congr. Fluid Mech.* **1997**, *2*, 557–560.
19. Khalili, A.; Shivakumara, I.S. Onset of convection in a porous layer with net throughflow and internal heat generation. *Phys. Fluids* **1998**, *10*, 315. [CrossRef]
20. Brevdo, L. Three-dimensional absolute and convective instabilities at the onset of convection in a porous medium with inclined temperature gradient and vertical throughflow. *J. Fluid Mech.* **2009**, *641*, 475–487. [CrossRef]
21. Shivakumara, I.S.; Sureshkumar, S. Convective instabilities in a viscoelastic fluid-saturated porous medium with throughflow. *J. Geophys. Eng.* **2007**, *4*, 104–115. [CrossRef]
22. Yadav, D. Numerical investigation of the combined impact of variable gravity field and throughflow on the onset of convective motion in a porous medium layer. *Int. Commun. Heat Mass Transf.* **2019**, *108*, 104274. [CrossRef]
23. Kiran, P. Throughflow and gravity modulation effects on heat transport in a porous medium. *J. Appl. Fluid Mech.* **2016**, *93*, 1105–1113. [CrossRef]

24. Bhadauria, S.; Kiran, P. Chaotic and oscillatory magneto-convection in a binary viscoelastic fluid under g-jitter. *Int. J. Heat Mass Transf.* **2015**, *84*, 610–624. [CrossRef]
25. Kiran, P. Throughow and g-jitter effects on binary fluid saturated porous medium. *Appl. Math. Mech.* **2015**, *36*, 1285–1304. [CrossRef]
26. Shinkumara, I.S.; Nanjundappa, C.E. Effects of quadratic drag and throughflow on double diffusive convection in a porous layer. *Int. Commun. Heat Mass Transf.* **2006**, *33*, 357–363. [CrossRef]
27. Reza, M.; Gupta, A.S. Magnetohydrodynamic thermal instability in a conducting fluid layer with throughflow. *Int. J. Non-Linear Mech.* **2012**, *47*, 616–625. [CrossRef]
28. Nield, D.A.; Kuznetsov, A.V. The effects of combined horizontal and vertical heterogeneity on the onset of convection in a porous medium with horizontal throughflow. *Int. J. Heat Mass Transf.* **2011**, *54*, 5595–5601. [CrossRef]
29. Yadav, D. The onset of Darcy-Brinkman convection in a porous medium layer with vertical throughflow and variable gravity field effects. *Heat Transf.* **2020**, *49*, 3161–3173. [CrossRef]
30. Kiran, P.; Bhadauria, S. Throughflow and rotational effects on oscillatory convection with modulation. *Nonlinear Stud.* **2016**, *23*, 439–455.
31. Gasser, R.D.; Kazimi, M.S. Onset of convection in a porous medium with internal heat generation. *J. Heat Transf.* **1976**, *98*, 49–54. [CrossRef]
32. Tveitereid, M. Thermal convection in a horizontal porous layer with internal heat sources. *Int. J. Heat Mass Transf.* **1977**, *20*, 1045–1050. [CrossRef]
33. Yadav, D.; Wang, J.; Jinho, L. Onset of Darcy-Brinkman convection in a rotating porous layer induced by purely internal heating. *J. Porous Media* **2017**, *20*, 691–706. [CrossRef]
34. Mahabaleshwar, U.S.; Basavaraja, D.; Wang, S.; Lorenzini, G.; Lorenzini, E. Convection in a porous medium with variable internal heat source and variable gravity. *Int. J. Heat Mass Transf.* **2017**, *111*, 651–656. [CrossRef]
35. Gholamalizadeh, E.; Pahlevanzadeh, F.; Ghani, K.; Karimipour, A.; Nguyen, T.K.; Safaei, M.R. Simulation of water/FMWCNT nanofluid forced convection in a microchannel filled with porous material under slip velocity and temperature jump boundary conditions. *Int. J. Numer. Methods Heat Fluid Flow* **2020**, *30*, 2329–2349. [CrossRef]
36. Heydari, A.; Akbari, O.A.; Safaei, M.R.; Derakhshani, M.; Alrashed, A.A.A.A.; Mashayekhi, R.; Ahmadi Sheikh Shabani, G.; Zarringhalam, M.; Nguyen, T.K. The effect of attack angle of triangular ribs on heat transfer of nanofluids in a microchannel. *J. Therm. Anal. Calorim.* **2018**, *131*, 2893–2912. [CrossRef]
37. Maleki, H.; Safaei, M.R.; Togun, H.; Dahari, M. Heat transfer and fluid flow of pseudo-plastic nanofluid over a moving permeable plate with viscous dissipation and heat absorption/generation. *J. Therm. Anal. Calorim.* **2019**, *135*, 1643–1654. [CrossRef]
38. Riahi, N. Non-linear convection in a porous medium with internal heat sources. *Int. J. Non-Linear Mech.* **1984**, *19*, 469–478. [CrossRef]
39. Rionero, S.; Straughan, B. Convection in a porous medium with internal heat source and variable gravity effects. *Int. J. Eng. Sci.* **1990**, *28*, 497–503. [CrossRef]
40. Du, Z.G.; Bilgen, E. Natural convection in vertical cavities with internal heat generating porous medium. *Heat Mass Transf.* **1992**, *27*, 149–155. [CrossRef]
41. Hewitt, G.F.; Shires, G.L.; Bott, T.R. *Process Heat Transfer*; CRC Press: Boca Raton, FL, USA, 1994.
42. Choi, E.; Chamkha, A.; Nandakumar, K. A bifurcation study of natural convection in porous media with internal heat sources: The non-Darcy effects. *Int. J. Heat Mass Transf.* **1998**, *41*, 383–392. [CrossRef]
43. Yadav, D.; Lee, J.; Cho, H.H. Brinkman convection induced by purely internal heating in a rotating porous medium layer saturated by a nanofluid. *Powder Technol.* **2015**, *286*, 592–601. [CrossRef]
44. Yadav, D.; Bhargava, R.; Agrawal, G.S. Boundary and internal heat source effects on the onset of Darcy–Brinkman convection in a porous layer saturated by nanofluid. *Int. J. Therm. Sci.* **2012**, *60*, 244–254. [CrossRef]
45. Barletta, A.; Celli, M.; Rees, D.A. The onset of convection in a porous layer induced by viscous dissipation: A linear stability analysis. *Int. J. Heat Mass Transf.* **2009**, *52*, 337–344. [CrossRef]
46. Sphaier, L.A.; Barletta, A.; Celli, M. Unstable mixed convection in a heated inclined porous channel. *J. Fluid Mech.* **2015**, *778*, 428–450. [CrossRef]
47. Vanishree, R.K. Effects of throughflow and internal heat generation on a thermo convective instability in an anisotropic porous medium. *J. Appl. Fluid Mech.* **2014**, *7*, 581–590.
48. Barletta, A.; Rossi di Schio, E.; Storesletten, L. Convective roll instabilities of vertical throughflow with viscous dissipation in a horizontal porous layer. *Transp. Porous Media* **2010**, *81*, 461–477. [CrossRef]